

## Investigation of the Leggett-Garg Inequality for Precessing Nuclear Spins

Vikram Athalye,<sup>1,\*</sup> Soumya Singha Roy,<sup>2,†</sup> and T. S. Mahesh<sup>2,‡</sup>

<sup>1</sup>*Department of Applied Physics, Cummins College of Engineering, Karvenagar, Pune 411052, India*

<sup>2</sup>*NMR Research Center, Indian Institute of Science Education and Research, Pune 411008, India*

(Received 12 February 2011; published 19 September 2011)

We report experimental implementation of a protocol for testing the Leggett-Garg inequality (LGI) for nuclear spins precessing in an external magnetic field. The implementation involves certain controlled operations, performed in parallel on pairs of spin-1/2 nuclei (target and probe) from molecules of a nuclear magnetic resonance ensemble, which enable evaluation of temporal correlations from an LG string. Our experiment demonstrates violation of the LGI for time intervals between successive measurements, over which the effects of relaxation on the quantum state of target spin are negligible. Further, it is observed that the temporal correlations decay, and the same target spin appears to display macro-realistic behavior consistent with LGI.

DOI: [10.1103/PhysRevLett.107.130402](https://doi.org/10.1103/PhysRevLett.107.130402)

PACS numbers: 03.65.Ta, 03.67.Ac, 76.30.-v, 76.60.-k

Distinguishing quantum from classical behavior has been an important issue since the development of quantum theory [1–5]. This issue is also at the heart of physical realizations of quantum information processing (QIP) [6]. Experimental tests for confirming quantumness in physical systems are usually guided by the Bell-type inequalities [2] and the Leggett-Garg inequality (LGI) [4]. Bell-type inequalities place bounds on certain combinations of correlation coefficients corresponding to measurement outcomes for spacelike separated systems which are assumed unable to influence one another (local realism). LGI, on the other hand, places bounds on combinations of temporal correlation coefficients between successive measurement outcomes for a system. Here, the system at any instant of time is assumed to be in one or the other of many possible states, and each measurement is assumed to be perfectly noninvasive, in the sense that it has no effect on the system's subsequent dynamics (macrorealism). In other words, violation of LGI indicates that the system's dynamics cannot be understood in classical terms. In recent years, various protocols for implementing LGI and its refined versions have been proposed and experimentally demonstrated [7].

In this Letter, we describe for the first time the implementation of LGI protocol for individual spin-1/2 nuclei [from a liquid nuclear magnetic resonance (NMR) sample] precessing in a magnetic field and interacting with their local environments. A typical spin-1/2 system is genuinely “microscopic” and exhibits quantum behavior. However, it is well-known that, due to decoherence, microscopic quantum systems appear to behave classically and as a consequence QIP tasks relying on such candidate systems tend to fail [8]. Nuclear spins from an NMR sample are examples of microscopic quantum systems that are in constant interaction with their local environment and are also candidate systems for QIP tasks. The interactions such as dipole-dipole and chemical-shift anisotropy are known

to be leading to decoherence, dissipation, and relaxation processes within the spin ensemble [9]. In experimental setups such as NMR, successful QIP implementation therefore demands confirmation of the “survival” of and determination of the “durability” of quantumness in candidate systems. While an LGI test was originally proposed for addressing the fundamental question about the ability of a macroscopic system to behave quantum mechanically, considering its basic mathematical framework, we extend such a test to investigate the survival and durability of quantumness within individual nuclear spins interacting with their environments. The investigation also sheds light on the possible consistency of the assumptions of macro-realism with the “decoherence perspective” [10].

Although individual nuclear spins from an NMR sample are not directly addressable, the sample provides an easily accessible ensemble of nuclear spins from a large number of molecules. Therefore, the experimental evaluation of a particular temporal correlation involves simultaneous implementations of the LGI protocol on a large number of nuclei (identical “targets”). Further, an NMR readout is an “ensemble average” obtained in terms of magnetization signal. One thus needs to relate the required temporal correlation from an LG string with the NMR signal. A quantum network for encoding correlation between measurement outcomes of a target system in the phase of a probe system has recently been proposed by Moussa *et al.* [11]. With this network, they were able to demonstrate quantum contextuality using nuclear spins from a solid state NMR sample. In this Letter, we exploit this network for testing LGI.

We report results for values of LG strings containing three and four temporal correlations as functions of delay between successive measurements. We have found good agreement between the quantum mechanically expected and experimentally observed values of the strings for short time scales over which the decay in correlations due to

typical NMR relaxation processes is ineffective. Further, to demonstrate the effect of decoherence on the state of individual target nuclei which leads to relaxation of the entire ensemble, we have also measured the values of LG strings over longer time scales and found that the LG strings gradually decay and ultimately fall within the classical bounds.

**Leggett-Garg inequality.**—Consider a system (the target) whose state evolution in time is governed by a particular Hamiltonian. To perform an LGI test for the system, a particular system observable (say,  $\mathbb{Q}$ ) that can be taken as “dichotomic,” i.e., having two possible states with measurement outcomes  $Q = \pm 1$ , requires to be identified. Next, from a set of  $n$  measurement instants  $\{t_1, t_2, t_3, \dots, t_n\}$ , pairs of instants  $t_i$  and  $t_j$ , such that  $j = i + 1$ , and a pair containing the first ( $i = 1$ ) and the last ( $j = n$ ) instants are to be chosen. For each such pair, one is then required to perform measurements of  $\mathbb{Q}$  on the target system at the corresponding two instants and obtain outcomes  $Q(t_i)$  and  $Q(t_j)$ . After repeating these two-time measurements over a large number of trials (say,  $N$ ), one can obtain the two-time correlation coefficient (TTCC)  $C_{ij}$  for each pair given by the formula

$$C_{ij} = \frac{1}{N} \sum_{r=1}^N Q_r(t_i) \cdot Q_r(t_j), \quad (1)$$

where  $r$  is the trial number. Finally, the values of these coefficients are to be substituted in the  $n$ -measurement LG string given by

$$K_n = C_{12} + C_{23} + C_{34} + \dots + C_{(n-1)n} - C_{1n}. \quad (2)$$

Each coefficient from the right-hand side of the above LG string would have a maximum value of +1 corresponding to perfect correlation, a minimum value of −1 corresponding to perfect anticorrelation, and 0 for no correlation. Thus, the upper bound for  $K_n$  consistent with macrorealism comes out to be  $(n - 2)$ ; the lower bound is  $-n$  for odd  $n$  and  $-(n - 2)$  for even  $n$ . With these considerations, the LGI reads  $-n \leq K_n \leq (n - 2)$  for odd  $n$  and  $-(n - 2) \leq K_n \leq (n - 2)$  for even  $n$ . For example,  $-3 \leq K_3 \leq 1$  and  $-2 \leq K_4 \leq 2$ .

**Spin-1/2 precession.**—The Zeeman Hamiltonian for the precession of a spin-1/2 nucleus in a magnetic field about the  $z$  axis is given by  $\hat{H} = \frac{1}{2} \omega \hat{\sigma}_z$ , with  $\omega$  being the angular precession frequency and  $\hat{\sigma}_z$  the Pauli  $z$  operator. For the present Letter, we choose the Pauli  $x$  operator, i.e.,  $\hat{\sigma}_x$ , as the dichotomic observable [12]. The quantum mechanical expression of  $C_{ij}$  for  $\hat{\sigma}_x$  measurements on the nucleus is given by [10]

$$C_{ij} = \langle \hat{\sigma}_x(t_i) \hat{\sigma}_x(t_j) \rangle \approx \cos\{\omega(t_j - t_i)\}. \quad (3)$$

In Heisenberg representation, one can obtain this relation by using the definition [13]

$$C_{ij} \approx \frac{1}{2} \sum_k \langle k | \hat{\sigma}_x(t_i) \hat{\sigma}_x(t_j) | k \rangle_z. \quad (4)$$

Here,  $|k\rangle_z \in \{|0\rangle, |1\rangle\}$  is an eigenstate of the Pauli  $z$  operator. If we divide the total duration from  $t_1$  to  $t_n$  into  $(n - 1)$  equal intervals of duration  $\Delta t$ , we can express the LG string consistent with Eq. (3) as

$$K_n = (n - 1) \cos\{\omega \Delta t\} - \cos\{(n - 1)\omega \Delta t\}. \quad (5)$$

The protocols for evaluating  $K_3$  and  $K_4$  are illustrated in Fig. 1. It can be seen that the quantum bounds for  $K_3$  and  $K_4$  are  $[-3, +1.5]$  and  $[-2\sqrt{2}, +2\sqrt{2}]$ , respectively.

**Evaluating TTCCs using the network proposed by Moussa et al.**—Suppose that we wish to evaluate correlations between the outcomes of repeated measurements of two commuting dichotomic unitary observables  $S_1$  and  $S_2$  for a target system ( $T$ ). Consider an ancilla qubit (called “probe”  $P$ ) and a unitary transformation for the joint system  $T + P$ ,

$$U_S = \mathbb{1}_P \otimes (P_+)_T + (\hat{\sigma}_z)_P \otimes (P_-)_T. \quad (6)$$

Here,  $P_+$  and  $P_-$  are the projectors onto the eigenspace of  $S \in \{S_1, S_2\}$ , such that  $S = (P_+)_T - (P_-)_T$ .

Using Eq. (6), it can be shown that the ensemble measurement of the probe gives correlation between successively measured commuting observables of the target. For evaluating TTCCs from an LG string, the observable set for the target qubit is  $\{\hat{\sigma}_x(t_i), \hat{\sigma}_x(t_j)\}$  and the corresponding unitaries to be applied to the joint  $(P + T)$  system at different time instants  $t_i < t_j$  are

$$U_{\hat{\sigma}_x}(t_q) = \mathbb{1}_P \otimes P_+(t_q) + (\hat{\sigma}_z)_P \otimes P_-(t_q). \quad (7)$$

Here,  $\hat{\sigma}_x(t_q) = P_+(t_q) - P_-(t_q)$  and  $q = i, j$  for time instants  $t_i$  and  $t_j$ . The quantum network for implementing these unitaries is shown in Fig. 2(a).

Let the target qubit  $T$  be initially prepared according to  $\rho$ . If the probe qubit  $P$  is initially in one of the eigenstates of the  $\hat{\sigma}_x$  operator, say,  $|+\rangle = (|0\rangle + |1\rangle)/\sqrt{2}$ , the density matrix of the joint system is given by

$$(\rho)_{P+T} = (|+\rangle\langle+|)_P \otimes (\rho)_T. \quad (8)$$

Because of the application of the unitaries (7), the joint density matrix evolves according to

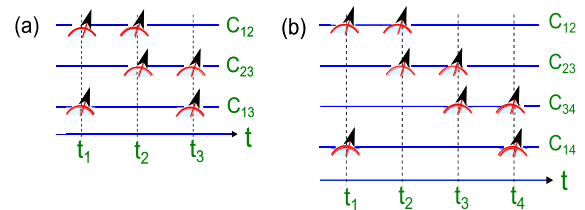


FIG. 1 (color online). The protocols for evaluating (a)  $K_3 = C_{12} + C_{23} - C_{13}$  and (b)  $K_4 = C_{12} + C_{23} + C_{34} - C_{14}$ .

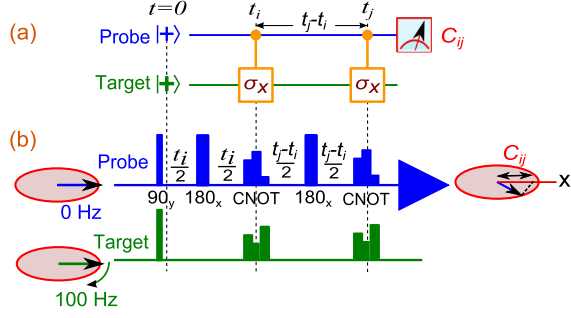


FIG. 2 (color online). Quantum network for the evaluation of (a) TTCCs and (b) the corresponding NMR pulse sequence. The ensemble was initially prepared according to  $(\rho)_P \otimes (\rho)_T$ , where  $(\rho)_P = (1 - \epsilon_P)\mathbb{1}/2 + \epsilon_P|+\rangle\langle+|$  and  $(\rho)_T = (1 - \epsilon_T)\mathbb{1}/2 + \epsilon_T|+\rangle\langle+|$ . Here,  $\epsilon_{P/T}$  is a dimensionless quantity which represents the purity of the initial states [13].

$$(\rho)_{P+T} \rightarrow U(t_j, t_i)(\rho)_{P+T}U^\dagger(t_i, t_j) = (\rho')_{P+T}, \quad (9)$$

where  $U(t_j, t_i) = U_{\hat{\sigma}_x}(t_j)U_{\hat{\sigma}_x}(t_i)$ . In terms of the evolved joint density matrix, the probabilities of obtaining  $\pm 1$  outcomes for the Pauli  $x$  measurements on the probe are given by

$$p(\pm 1) = \text{tr}_{P+T}[(\rho')_{P+T}\{(|\pm\rangle\langle\pm|)_P \otimes \mathbb{1}_T\}]. \quad (10)$$

By tracing over the probe states and using Eqs. (7)–(9) in Eq. (10), one obtains

$$p(\pm 1) = \text{tr}_T[\{P_+(t_i)P_\pm(t_j) + P_-(t_i)P_\mp(t_j)\}(\rho)_T]. \quad (11)$$

The ensemble average of the measurement outcome of the joint  $(P + T)$  observable is given by

$$\langle(\hat{\sigma}_x)_P \otimes \mathbb{1}_T\rangle = +p(+1) - p(-1). \quad (12)$$

Substitution of the results (11) into Eq. (12) gives

$$\begin{aligned} \langle(\hat{\sigma}_x)_P \otimes \mathbb{1}_T\rangle &= \text{tr}_T[\hat{\sigma}_x(t_i)\hat{\sigma}_x(t_j)(\rho)_T] \\ &= \langle\hat{\sigma}_x(t_i)\hat{\sigma}_x(t_j)\rangle = C_{ij}. \end{aligned} \quad (13)$$

Comparing Eqs. (3) and (13), it is clear that each TTCC in an LG string can be evaluated by applying unitaries (7) to the joint (probe + target) system followed by an ensemble measurement of the Pauli  $x$  operator on the probe.

**Experiment.**—The NMR sample consisted of 2 mg of  $^{13}\text{C}$  labeled chloroform ( $^{13}\text{CHCl}_3$ ) dissolved in 0.7 ml of deuterated dimethyl sulphoxide. To implement the protocol described above, the spin-1/2 nuclei of  $^{13}\text{C}$  and  $^1\text{H}$  atoms are treated as the target spin and the probe spin, respectively. All the experiments are carried out on a Bruker 500 MHz spectrometer at an ambient temperature of 300 K. The carbon rf offset was chosen such that the  $^{13}\text{C}$  spin precesses at an angular frequency of  $\omega = 2\pi \times 100$  rad/s under the effective longitudinal field in the rotating frame of the rf. The proton rf offset was chosen at the resonance frequency of the  $^1\text{H}$  spin. The indirect spin-spin coupling constant ( $J$ ) for these two spins is

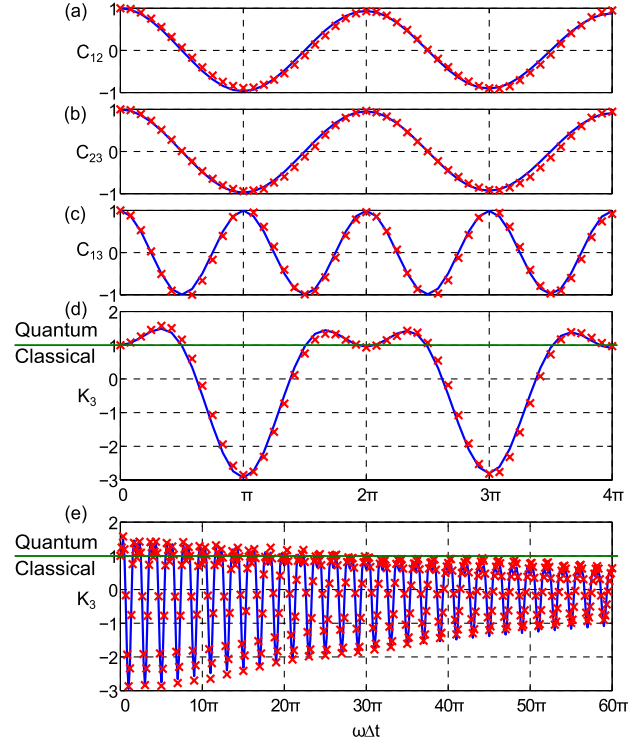


FIG. 3 (color online). Correlations versus  $\Delta t$ : (a)  $C_{12}$ , (b)  $C_{23}$ , and (c)  $C_{13}$ .  $K_3$  is plotted for the ranges (d)  $\omega\Delta t \in [0, 4\pi]$  and (e)  $\omega\Delta t \in [0, 60\pi]$ . Continuous lines are theoretical fits ( $K_3$  with decay) to the experimental data points (crosses).

217.6 Hz. The spin-lattice ( $T_1$ ) and spin-spin ( $T_2$ ) relaxation time constants for the  $^1\text{H}$  spin are, respectively, 4.1 and 4.0 s. The corresponding time constants for  $^{13}\text{C}$  are 5.5 and 0.8 s.

The NMR pulse sequence for evaluating TTCCs is described in Fig. 2(b). Initial  $90^\circ$   $y$  pulses on both probe and target prepare them in  $\hat{\sigma}_x$  states. All the spin manipulations, including the C-NOT gates corresponding to the  $U_{\hat{\sigma}_x}$  operation, are realized by specially designed strongly modulated pulses [14] having Hilbert-Schmidt fidelity of over 0.995. These rf pulses are designed to be robust against the rf field inhomogeneity in the range of 90% to 110% and static field inhomogeneity in the range of  $-5$  Hz to  $+5$  Hz. The evolution of  $J$  coupling during the intervals between the measurements is refocused using  $\pi$  pulses on the  $^1\text{H}$  spin. Collective transverse magnetization of the probe spins induces an observable electromotive force on a resonant Helmholtz-type coil which is amplified, digitized, and stored as the probe signal. Quadrature detection of the probe signal enables us to measure the  $x$  component of the probe magnetization as the real part of the complex signal. After the Fourier transform, the probe signal is fitted to a mixed Lorentzian line shape to extract the absorptive content. A reference signal was obtained by an identical experiment with  $\Delta t = 0$ . The correlation  $C_{ij}(\Delta t)$  was measured at each value of  $\Delta t$  by normalizing the real part of the probe signal with the reference signal.

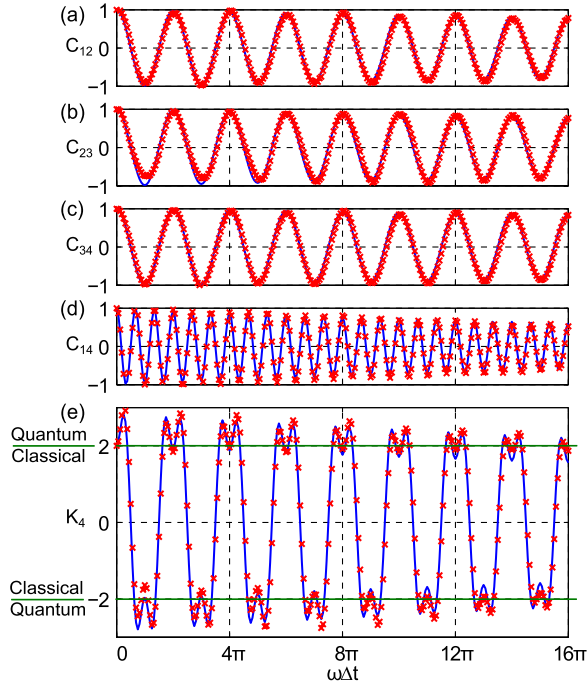


FIG. 4 (color online). The individual correlations  $C_{12}$ ,  $C_{23}$ ,  $C_{34}$ , and  $C_{14}$  are plotted in (a)–(d), and  $K_4$  is plotted in (e).

The three-measurement LG string  $K_3 = C_{12} + C_{23} - C_{13}$  was evaluated for  $\omega\Delta t$  varying from 0 to  $60\pi$ , with  $\Delta t$  incremented from 0 to 300 ms in 360 equal steps. The results of the experiment are shown in Fig. 3. The maximum random errors in these experiments were found to be about  $\pm 0.005$ . It is clearly seen that the experimental  $K_3$  data points violate the classical limit and hence macrorealism. Figure 3(e) shows the  $K_3$  plot for an extended duration consisting of 30 periods. It can be observed that the experimental values of  $K_3$  gradually decay at a time constant of about 288 ms predominantly due to  $T_1$  and  $T_2$  relaxations and due to inhomogeneities in the magnetic field, thus eventually falling within the classical limit for  $\omega\Delta t > 26\pi$  ( $\approx 42$  ms).

Similarly, the four-measurement LG string  $K_4$  was measured for  $\omega\Delta t$  varying from 0 to  $16\pi$  (i.e., for 8 periods), with  $\Delta t$  varying from 0 to 80 ms. The results of the experiment are shown in Fig. 4. Unlike the three-measurement case, where the classical and quantum mechanical lower limits for  $K_3$  values match (i.e.,  $-3$ ), the four-measurement case displays violation of the classical limit both in the positive as well as in the negative sides. Similar to the previous case, we observe an exponential decay of  $K_4$  with a time constant of about 324 ms. Decay of LG strings is faster than the measured  $T_2$  values of either spin mainly because  $T_2$ 's have been measured using Carr-Purcell-Meiboom-Gill sequences which suppress the effects of static field inhomogeneity and local fluctuating fields.

**Conclusion.**—The present investigation of LGI employs an ensemble of nuclear spins and alleviates the need for

repeated experiments on single isolated systems [11]. Simultaneous implementation of controlled operations on target-probe pairs enables evaluation of TTCCs and hence plotting of LG strings as functions of two-time measurement delays. The plots exhibit both violation and satisfaction of LGI, respectively, for delays shorter than and comparable to the relaxation time scales. Although a detailed theoretical explanation of our results goes beyond the scope of the present Letter, we qualitatively interpret them as follows: For time scales, over which environmental effects on spin states are negligible, individual target spins can be taken as isolated quantum systems. The plots do reflect this fact in terms of violation of LGI. However, the spin-environment interaction tends to destroy the phase relationship characterizing the superposition of quantum states of the target nuclear spin. As a result, each member from the ensemble, with its respective environment traced out, begins to appear as if preexisting in either one of the two states (of a spin observable chosen for performing measurements, which is Pauli  $x$  in the present Letter) but not in their superposition. Such a gradual transition from quantum to macrorealistic behavior of individual microscopic systems manifests itself in terms of decay of TTCCs. This ultimately leads to the satisfaction of LGI. Our experimental results thus not only demonstrate initial macrorealism-violating dynamics in genuine microscopic systems such as individual nuclear spins, but also bring forward their environment-induced emergent macrorealistic behavior, captured in terms of satisfaction of LGI and consistent with the decoherence mechanism.

The authors gratefully acknowledge discussions with Professor Anil Kumar (IISc, Bangalore), Professor A. Leggett (University of Illinois, UC), and Professor Arvind Kumar (HBCSE, Mumbai).

*Note added in proof.*—After submission of this paper, violation of LGI for the three-measurement case has been reported by Souza *et al.* [15]

\*vikathalye@gmail.com

†ss.roy@iiserpune.ac.in

\*mahesh.ts@iiserpune.ac.in

- [1] A. Einstein, B. Podolsky, and N. Rosen, *Phys. Rev.* **47**, 777 (1935).
- [2] J. S. Bell, *Rev. Mod. Phys.* **38**, 447 (1966).
- [3] S. Kochen and E. P. Specker, *J. Math. Mech.* **17**, 59 (1967).
- [4] A. J. Leggett and A. Garg, *Phys. Rev. Lett.* **54**, 857 (1985).
- [5] N. D. Mermin, *Rev. Mod. Phys.* **65**, 803 (1993).
- [6] M. A. Nielsen and I. L. Chuang, *Quantum Computation and Quantum Information* (Cambridge University Press, Cambridge, England, 2002).
- [7] R. Ruskov, A. N. Korotkov, and A. Mizel, *Phys. Rev. Lett.* **96**, 200404 (2006); A. N. Jordan, A. N. Korotkov, and M. Buttiker, *ibid.* **97**, 026805 (2006); N. S. Williams and A. N. Jordan, *ibid.* **100**, 026804 (2008); M. E. Goggin *et al.*, *Proc. Natl. Acad. Sci. U.S.A.* **108**, 1256 (2011);



- M. Wilde and A. Mizel, [arXiv:quant-ph/1001.1777v2](#); A. Palacios-Laloy *et al.*, *Nature Phys.* **6**, 442 (2010); J. Dressel *et al.*, *Phys. Rev. Lett.* **106**, 040402 (2011).
- [8] M. A. Schlosshauer, *Decoherence and the Quantum-to-Classical Transition* (Springer-Verlag, Berlin, 2007).
- [9] J. Kowalewski and L. Maler, *Nuclear Spin Relaxation in Liquids: Theory, Experiments, and Applications* (Taylor & Francis, London, 2006).
- [10] J. Kofler and C. Brukner, *Phys. Rev. Lett.* **99**, 180403 (2007).
- [11] O. Moussa *et al.*, *Phys. Rev. Lett.* **104**, 160501 (2010).
- [12] See Supplemental Material at <http://link.aps.org/supplemental/10.1103/PhysRevLett.107.130402> for confirmation of the dichotomic nature of the  $x$  component of the nuclear spin observable.
- [13] The initial state is highly mixed with a purity factor of  $10^{-4}$ , justifying the approximate equalities in expressions (3) and (4).
- [14] E.M. Fortunato *et al.*, *J. Chem. Phys.* **116**, 7599 (2002); T.S. Mahesh and D. Suter, *Phys. Rev. A* **74**, 062312 (2006).
- [15] A.M. Souza, I.S. Oliveira, and R.S. Sarthour, *New J. Phys.* **13**, 053023 (2011).